

V.D. Nguyen, J. Dickinson, J. Lemay,  
D. Provençal, Y. Jean and Y. Chalifour  
Departements of Mechanical and Electrical Engineering,  
Laval University, Ste-Foy, Quebec, Canada G1K 7P4

### Abstract

Skin friction measurements have been made behind flat plate turbulence manipulators using four servo-controlled balances. The observed region downstream of the manipulator has been extended to  $150 \delta_i$ , where  $\delta_i$  is the boundary layer thickness at the manipulator station. For the single element configuration, the results confirmed all the trends observed by Mumford and Savill, with an optimum height of the manipulator around  $0.75 \delta_i$ . For the twin element configurations tested, the best skin friction reduction results were obtained with the ribbons located at  $0.38$  and  $0.76 \delta_i$ . The trend of the present direct skin friction data is in agreement with that of the Cavendish Laboratory group and supports the contention, based on their visualisation work, that the existence of an influencing wake interacting with the boundary layer hairpin vortices, provides the main mechanism for the reduction of skin friction.

### Nomenclature

y	distance normal to the wall
$\delta$	boundary layer thickness
$\delta_i$	boundary layer thickness at the manipulator station
u	measured velocity at y
$U_e$	free stream velocity
$U_T$	skin friction velocity = $(\tau_w/\rho)^{1/2}$
$U_+$	= $u/U_T$
$Y_+$	= $y U_T/\nu$
$\nu$	air kinematic viscosity
$\tau_w$	wall shear stress
$C_f$	skin friction coefficient
$\rho$	air density
$Re_\theta$	Reynolds number based on the momentum thickness
$\alpha$	correction factor for the displacement effect
t	thickness of the turbulence manipulator
$\ell$	chord length of the turbulence manipulator
x	distance between the trailing edge of the manipulator and a particular position downstream
h	height of the manipulator

### 1. Introduction

Encouraged and intrigued by preliminary results obtained during wind tunnel tests in the year 1982-83, and published at the 1984 AIAA Congress in Reno [1], we decided to carry out further studies on viscous drag reduction using thin, transverse blades, termed LEBU's, or "Large Eddy Break-Up devices", by the research group at NASA - Langley [2,3,4]. During the month of February 1984, whilst our present tests were continuing, we received a most interesting article from Dr. Savill of Cambridge University [5]. The work of the Cavendish Laboratory Group was particularly

welcome in so far as it indicated identical trends in skin friction patterns measured both with their large ( $177 \text{ cm}^2$ ) floating element balance and our own much smaller ( $6.4 \text{ cm}^2$ ) servo-controlled units, and for the light it threw on the whole physical structure of the flows.

We are now convinced that the term LEBU is not really appropriate, in the light of the results of Mumford and Savill's visualisation studies [5]. Indeed the latter clearly demonstrate that the wake behind the "turbulence manipulator" plays a far more predominant role. We have already had some suspicions about the influence of the wake from the form of the velocity profiles and  $C_f$  variations behind the blades [1], but had never thought that such a wake could provide a primary mechanism for reducing skin friction by promoting such an active interaction between the wake vortices and the boundary layer hairpin vortices. We thus decided that the present title is more appropriate than that registered in the Preliminary Programme of the Congress.

Our work is not yet at the stage of being a systematic parametric study, but it is hoped that it may provide complementary data to more detailed investigations presently being carried out by a number of international research groups. The data we would like to present consist of local skin friction measurements using four servo-controlled floating element balances behind two different thin blade configurations, consisting of both single and double blades placed at different heights from the wall. The range of measurements has also been extended downstream to some 150 times the boundary layer thickness at the station occupied by the blades.

### 2. Experimental facilities and testing conditions

#### 2.1 Wind tunnel and instrumentation

The low speed wind tunnel (fig. 1) used in this investigation is basically the same as that employed in our earlier experiments [1], being an open type with a variable speed, solid state drive control. The cross-section is  $610 \times 460 \text{ mm}$  ( $24" \times 18"$ ) and an additional section has been added, bringing the total length of the test section up to approximately 4 metres. The floor of the wind tunnel, on which the boundary layer develops, is equipped with three new aluminium test plates. These new plates contain static pressure taps, 15 inserts for the skin friction balances and 9 inserts for the flush hot-wires (for a future investigation). The turbulence manipulator is placed at 880 mm from the end of the 5:1 entry contraction, and both its position and the

different measuring stations are shown in figure 2 and in the following table :

stations	1	2	3	4	5
x(m)	0.165	0.544	0.724	0.904	1.084
	6	7	8	9	10
	1.264	1.738	1.918	2.098	2.278
	11	12	13	14	15
	2.458	2.935	3.187	3.295	3.475
	16				
	3.655				

Tests were carried out at a nominal free stream velocity around 16.5 m/s. Since the thickness of the tripped boundary layer was fairly large, even at the beginning of the test section, we decided to take out the 3.2 mm (1/8") diameter rod originally placed at the end of the contraction [1]. This gave us a boundary layer thickness of around 25.4 mm (1") at station 1 and of 64 mm (2.52") at station 15, corresponding respectively to the free stream velocities of 16 m/s and 17 m/s. The Reynolds number based on the momentum thickness  $R_\theta$  varies from 2900 at station 1 to 6750 at station 15, which is quite acceptable for an eventual comparison with the results of the other groups.

Before carrying out tests with the balances, a survey was made of the static pressure variation along the test section, indicating the weak favorable pressure gradient illustrated in figure 7.

Skin friction measurements were made with one single headed servo-controlled balance and three twin-headed differential balances described briefly in the following section. A 0.8 mm ( $d = 0.032$ ") diameter pitot tube was used in conjunction with the static pressure holes at the wall to measure the velocity profiles. The same electronic circuit used in the previous experiment was again employed to detect when the probe touched the wall, to a nominal accuracy of 0.02 mm. The only corrections made to the velocity data were those due to the "displacement effect" and the usual correction factor of  $\alpha = 0.15$  was taken (i.e.  $\Delta y = \alpha \cdot d$ ).

All the velocity data were averaged by feeding the signals of the pressure transducers to a very economical data acquisition system developed by the fourth author using a SINCLAIR ZX-81 micro-computer. The outputs of the skin friction balances were read directly from their own D.V.M.'s, the electronic control units being equipped with their own passive filters (cf. fig. 6).

## 2.2 Skin friction balances

Four servo-controlled skin friction balances were used in the present series of tests; three of the differential type with twin floating heads (fig. 4) and the fourth a single-headed balance similar to the older versions illustrated in figure 5. A fairly detailed description and discussion of the balances has been given in reference [1], so we will restrict ourselves to a brief resumé of their construction and characteristics.

All the instruments consist basically of a light ( $\approx 1.5$  gm) floating head assembly, 25.4 mm (1") to 28.6 mm (1 1/8") in diameter, supported by four specially designed flexures forming a hinged parallelepiped, stiff in both the transverse direction and over most of its length, but extremely sensitive to small forces in the longitudinal direction. Attached to the moving assembly, just below the head, are the core of a linear voltage differential transformer (LVDT), and the coil of a small linear permanent magnet rotor. Under the action of an applied force the whole moving assembly starts to move. This movement is sensed by the LVDT, with an oscillator frequency of 20 kHz, whose output is demodulated and fed through correction networks, filters and an integrator, to the coil of the linear motor which provides the restoring force necessary to hold the "moving" assembly in the null position. Basically the motor acts like a loudspeaker in reverse, with coil current continually varying to compensate for the sum of all the perturbation forces (i.e. skin friction, vibration, inclination, acceleration).

A high closed loop gain allows the use of very small gaps (0.02 to 0.07 mm). Adjustment screws also permit a delicate centering and alignment of the head in the balance casing. The latter can then be "plugged" into holes (76 mm in diameter; 3") at the various measuring stations along the test section, and held in place by retaining rings which slip over the underside of the balance case.

The instruments are calibrated very simply by treating them as ordinary servo-controlled "weighing" balances, mounting them vertically and attaching weights to the floating head. The coil current varies linearly with applied force, and the corresponding voltage (1 mv  $\sim$  1 mg) is read-off on the front panel of the electronic control unit (fig. 6), which is also equipped with zero adjustments and filters. The balances are accurate to better than 1%, or 1 mg in the lower range (0 - 100 mg), and have a sensitivity of about 0.1 mg.

The twin-headed balance illustrated in figure 4 has been designed, hopefully, for use in slowly varying ( $< 30$  Hz) unsteady flows. By taking the differential output between the two channels, corresponding to the primary head and an identical dummy head hidden inside the balance case, it is possible to eliminate almost all (98%) parasitic effects such as inclination, vibration or acceleration. In the present tests however the outputs of both the single and differential balances were highly filtered since our immediate concern was to obtain mean data.

## 2.3 The turbulence manipulators

The turbulence manipulators used in this second experiment were the same as those described in our first tests [1]. They were made of horizontal plates, 0.4 mm thick, with a chord length of 19 mm. At the position they occupied, we obtained the following parameters :  $\frac{t}{\delta_i} \approx 0.017$  and  $\frac{l}{\delta_i} \approx 0.76$ .

The bands were stretched parallel to the floor of the wind tunnel in the spanwise direction using the device shown in figure 3. Two manipulator configurations were chosen. The first consisted

of a single ribbon placed at four different distances from the wall defined as follows ( $\delta_i \approx 25$  mm) :

$$\frac{h}{\delta_i} : 0.30, 0.47, 0.76 \text{ and } 1.02$$

The second configuration consisted of two parallel plates located at different positions giving the three following combinations :

$$\frac{h}{\delta_i} : 0.09 \text{ \& } 0.30, 0.30 \text{ \& } 0.52, \text{ and } 0.38 \text{ \& } 0.76.$$

### 3. Results and discussion

A check on the normal operation of the skin friction balances was made without any moderator. Balance data was registered at stations 1 and 15, and the results compared with those obtained using a Preston tube ( $d = 0.032$  , in diameter) in conjunction with V.C. Patel's calibration formula [6]. Agreement between the Preston tube and the balance data was excellent, the greatest difference being less than 3%, and this assured us that the balances were functioning satisfactorily. Typical wall law data, with the skin friction determined by the balances, without the moderator, closely satisfied the classical "universal" logarithmic wall law (cf. figure 8) :

$$u_+ = 5.5 \log y_+ + 5.5$$

The four balances were employed in turn at each of the measuring stations, providing mutually consistent data. The skin friction results presented in this paper represent the average of these readings.

The skin friction coefficient variation  $C_{f0}$ , without the manipulator, is shown in figure 9. All subsequent skin friction data were normalized with respect to  $C_{f0}$ , giving a direct indication of the skin friction reduction, as represented in figures 10, 11, 12 and 13 for the single blade configuration. Peak reductions of approximately 15%, 10%, 8% and 4% were recorded at downstream positions ( $x$ ) of around 7, 30, 40 and 70 times the initial boundary layer thickness ( $\delta_i$ ), respectively at height ratios ( $h/\delta_i$ ) of 0.3, 0.47, 0.76 and 1.02 (cf. figs. 10 to 13). In order to assess the optimum height of the manipulator, the areas under the previous smoothed curves were integrated using a planimeter. The results illustrated in figure 14 indicated an optimum value ( $h/\delta_i$ ) of around 0.75, with an average skin friction reduction of about 4% over 140 initial boundary layer lengths. The general results seem to confirm the trends observed by the Cambridge group. Any detailed comparisons are however a little premature until we have amassed more data, covering a wider range of manipulator geometries and tunnel speeds. A brief test at  $h/\delta_i = 0.3$ , shimming the blade to give it a small positive angle of attack ( $\sim 5^\circ$ ), did seem to indicate a drop in blade efficiency (fig. 10).

The data does suggest a small but significant reduction (1 to 2%) in  $C_f$  even very far downstream. It must be noted however that the total drag forces on the floating heads at the present tunnel test speed ( $\sim 16$  m/s) were around 30 milligrammes. A discrepancy of 1 mg therefore already represents a

3% in  $C_f$ , so a series of more detailed and repetitive tests are certainly required.

The skin friction data for the twin plate configuration are illustrated in figure 15. They indicated in all cases a long downstream influence of the turbulence manipulators, with  $h/\delta_i = 0.38$  and 0.76 providing the best overall skin friction reduction ( $\sim 6\%$ ).

### Concluding remarks

We are presently preparing for a much more detailed and intensive series of tests. An I.B.M. Personal Computer has been equipped with a 15 channel 12 bit A/D converter and will be used to control both tunnel speed and a traversing mechanism, and to store, average and analyse data. A larger number of balances are being built to cover the whole test section. Tests will include direct skin friction data with the balances, complementary indirect data using flush mounted hot-wire probes, pitot tube mean velocity traverses, and cross-wire measurements to start looking at modifications to the turbulent structure.

### Acknowledgements

We would like to express our thanks to all the undergraduate and graduate students who benevolently gave their time and energy to this project; to our workshop technicians for some beautiful machining and instrumentation work, and to our secretary for always cheerfully putting up with our last minute midnight typing requests.

### References

- [1] V.D. Nguyen, J. Dickinson, Y. Jean, Y. Chalifour, J. Anderson, J. Lemay, D. Haeberle, G. Larose - "Some experimental observations of the law of the wall behind large-eddy breakup devices using servo-controlled skin friction balances" - AIAA 22nd Aerospace Sciences Meeting, Reno, Nevada, January 9-12, 1984, Paper No AIAA-84-0346.
- [2] J.N. Hefner, J.B. Anders, D.M. Bushnell - "Alteration of outer flow structures for turbulent drag reduction" - AIAA 21st Aerospace Sciences Meeting, Reno, Nevada, Jan. 10-13, 1983, Paper No AIAA-83-0293.
- [3] D.M. Bushnell - "Turbulent drag reduction for external flows" - AIAA 21st Aerospace Sciences Meeting, Reno, Nevada, Jan. 10-13, 1983, Paper No AIAA-83-0227.
- [4] J.B. Anders, J.N. Hefner, D.M. Bushnell - "Performance of large-eddy breakup devices at post-transitional Reynolds numbers" - AIAA 22nd Aerospace Sciences Meeting, Reno, Nevada, Jan. 9-12, 1984, Paper No AIAA-84-0345.
- [5] J.C. Mumford, A.M. Savill - "Parametric studies of flat plate, turbulence manipulators including direct drag results and laser flow visualisation" - Proceedings of the ASME New-Orleans Conference, February 11-17, 1984.
- [6] V.C. Patel - "Calibration of the Preston tube and limitation on its use in pressure

gradients" - J. Fluid Mech., Vol. 23,  
pp. 185-208, 1965.

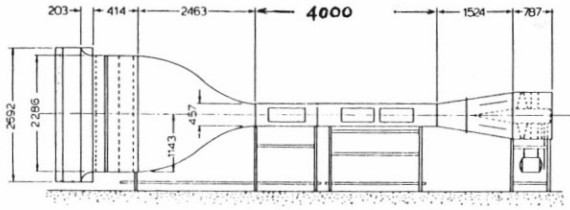


Fig. 1 The Laval 24" x 18" low speed wind tunnel (dimensions in mm)

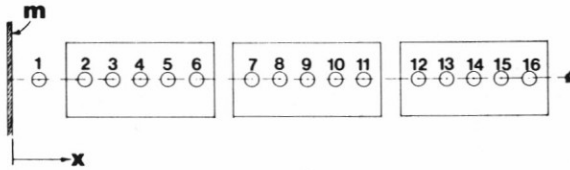


Fig. 2 Location of the measuring stations  
(m = turbulence manipulator)  
(Cf. table section 2.1)

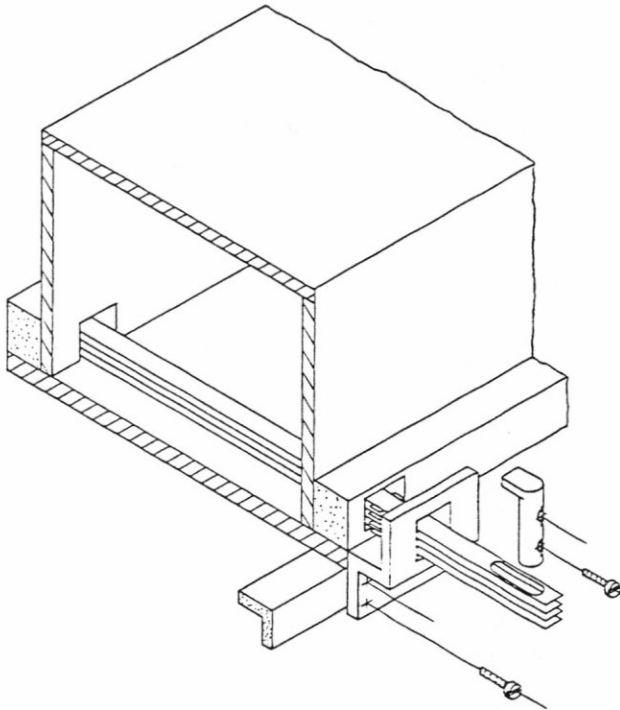


Fig. 3 The turbulence manipulators  
and stretching device

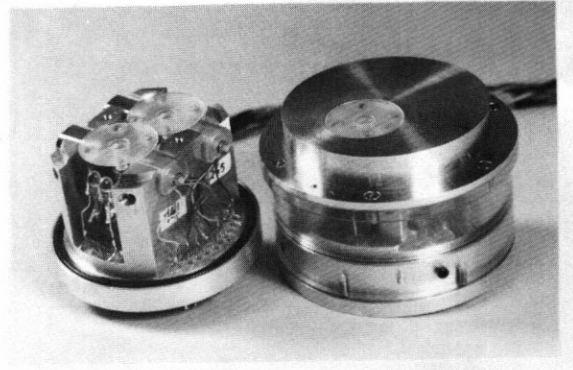


Fig. 4 Side view of twin headed dif-  
ferential skin friction balance  
(1 1/8" dia. head)

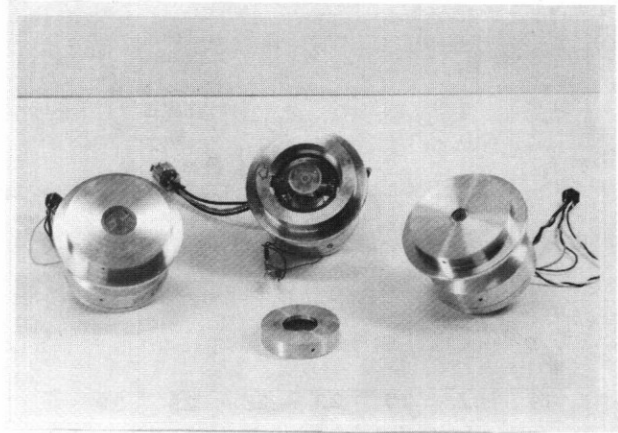


Fig. 5 Single-head servo-controlled skin  
friction balances : left and centre  
1" dia. floating heads, right 1/2" dia-  
meter

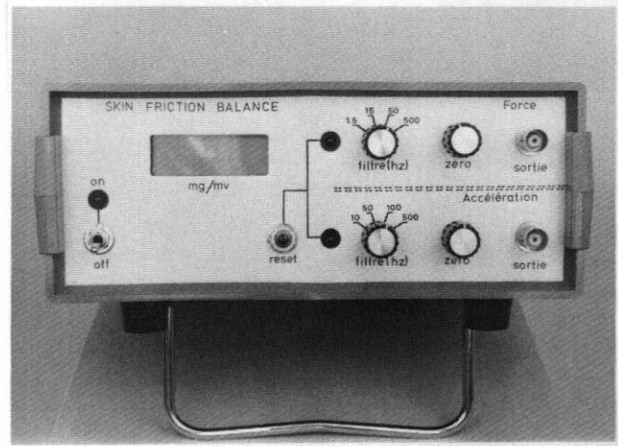


Fig. 6 Skin friction balance  
control unit

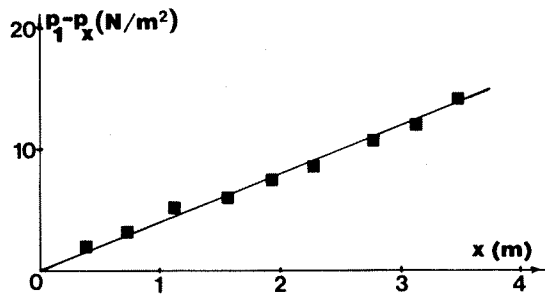


Fig. 7 Longitudinal static pressure variation

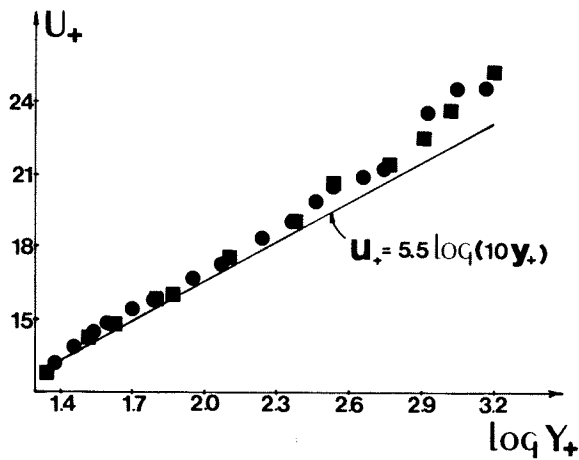


Fig. 8 The law of the wall without turbulence manipulator at stations 1 and 15 ● station 1 ■ station 15

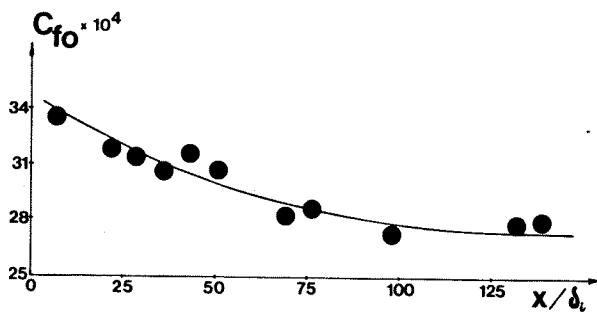


Fig. 9 Variation of local skin friction coefficient without turbulence manipulator

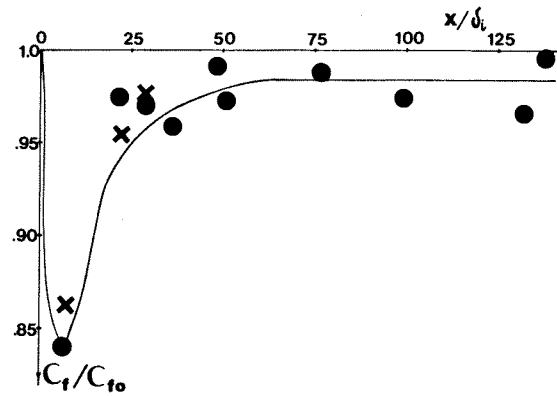


Fig. 10 Variation of local skin friction coefficient for single ribbon at  $\frac{h}{\delta_i} = 0.30$  (x : with shim giving a positive angle of attack of around  $5^\circ$ )

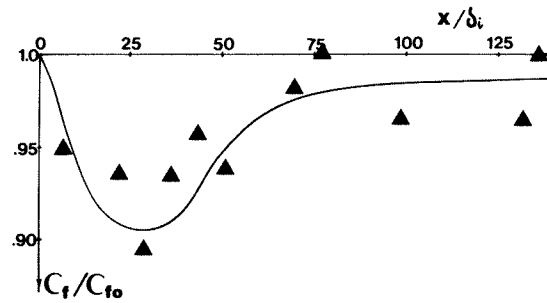


Fig. 11 Variation of local skin friction coefficient for single ribbon at  $\frac{h}{\delta_i} = 0.47$

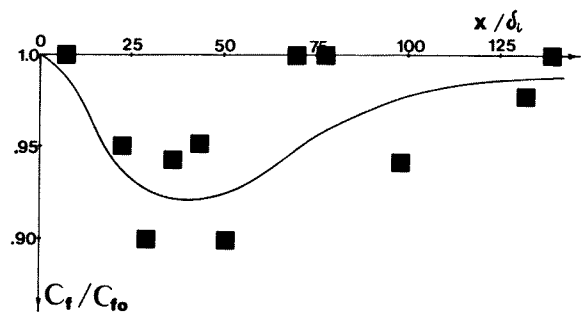


Fig. 12 Variation of local skin friction coefficient for single ribbon at  $\frac{h}{\delta_i} = 0.76$

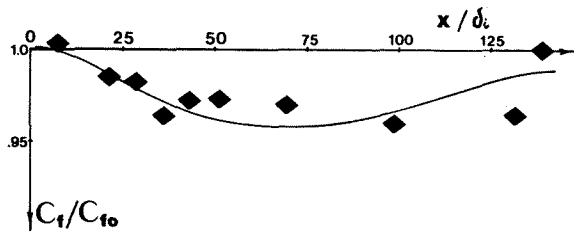


Fig. 13 Variation of local skin friction coefficient for single ribbon at  $\frac{h}{\delta_i} = 1.02$

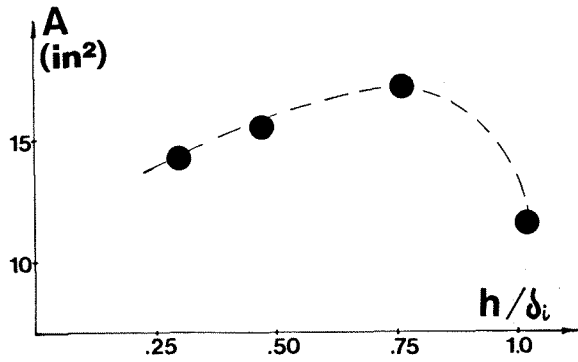


Fig. 14 Area under the smoothed curves of local skin friction variation versus turbulence manipulator height (15 in<sup>2</sup> corresponds to an average skin friction reduction of 3.5% over  $140 \delta_i$ ).

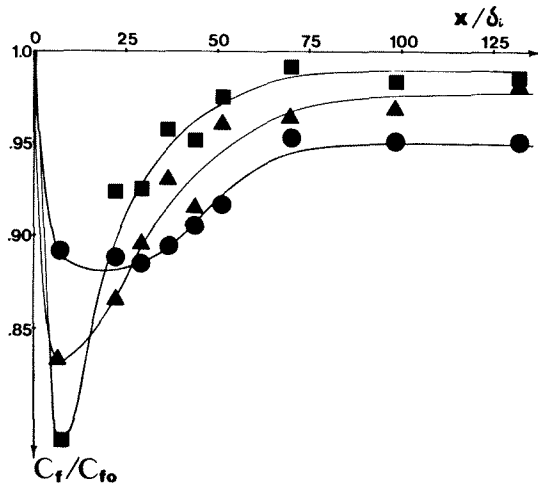


Fig. 15 Variation of local skin friction coefficient for twin plate configuration

$h/\delta_i$

- 0.38 and 0.76
- 0.09 and 0.30
- ▲ 0.30 and 0.52